

Original article

<https://doi.org/10.15828/2075-8545-2023-15-2-152-163>

CC BY 4.0

Effect of Laser Modification on Composite Films with Nanodispersed SiO₂

Natalia I. Cherkashina* , Vyacheslav I. Pavlenko , Andrey I. Gorodov , Daria A. Ryzhikh , Elena V. Forova 

Belgorod State Technological University named after V.G. Shukhov, Belgorod, Russia

* Corresponding author: e-mail: natalipv13@mail.ru

ABSTRACT: Introduction. This research is aimed at studying the effect of laser modification on composite films obtained on the basis of polyimide track (nuclear) membranes and filled with nanodispersed SiO₂ to change their optical and structural properties. **Materials and research methods.** Polyimide track (nuclear) membranes were used as a polymer matrix. Track diameter is 200 nm, membrane thickness is 25 μm. The tracks were filled with nanosized SiO₂ by hydrolysis of tetraethoxysilane in the presence of track membranes. For composite film surface modification, we used ytterbium pulsed fiber laser Minimarker 2-20 A4 PA. We studied the change in the surface microscopy of composite films, their optical density, IR-Fourier spectra and surface wettability depending on laser treatment. **Results and discussion.** The authors have found the possibility of creating a composite film based on a polyimide track (nuclear) membrane and nanodispersed SiO₂ by hydrolysis of tetraethoxysilane in the presence of a membrane. It is shown with the energy dispersive analysis method that silicon oxide has completely filled the pore volume of the track membrane. Laser modification of the composite material surface (composite film) leads to an increase in the contact angle of wetting from $\theta = 66.75 \pm 1.55^\circ$ to $\theta = 101.52 \pm 3.03^\circ$. Thus, the material acquires hydrophobic properties. Also, the laser films modification has a positive effect on the transmittance of the films, namely, this coefficient increases. The greatest change is observed in the infrared region of emitted spectrum, the average increase in transmission is +70.48%. **Conclusion.** The obtained results of the study are of great importance for understanding the mechanisms of creating composite films with improved optical properties, which can later be used to create composite films with desired optical properties for various applications.

KEYWORDS: composite film, track membrane, nanosized SiO₂, laser processing, optical properties, modification, contact angle of wetting.

ACKNOWLEDGMENTS: The study was funded by grant of the Russian Science Foundation No. 19-79-10064 (extension), <https://rscf.ru/project/19-79-10064/> with equipment based on the Center for High Technologies of the BSTU named after V.G. Shukhov.

FOR CITATION: Cherkashina N.I., Pavlenko V.I., Gorodov A.I., Ryzhikh D.A., Forova E.V. Effect of Laser Processing on Composite Films with Nanodispersed SiO₂. *Nanotechnologies in construction*. 2023; 15(2): 152–163. <https://doi.org/10.15828/2075-8545-2023-15-2-152-163>. – EDN: HWIKQS.

INTRODUCTION

Polyimides are a class of high-performance polymers containing imide groups. Their advantages: high mechanical properties, thermal stability in a wide temperature range (from -250°C to $+350^\circ\text{C}$), resistance to ultraviolet radiation and high chemical resistance [1–4]. Polyimides are useful in the aviation and space industries, nuclear power energy, electronics, solar cells, reflection devices, as mirror substrate material with a low surface density [5, 6]. From polymers, including polyimides, track membranes are made (translucent thin films with a smooth surface) [7, 8]. To obtain track (nuclear) mem-

branes, a polymer film is exposed to irradiation with heavy accelerated ion beams and chemical etching; the pore size will depend on the intensity, energy, and selected etching modes [9–11]. Track membranes occupy a special place in the medicine [12–15]. Furthermore, track membranes are used for ultrafiltration, media concentration in industry, and for the creation of polymer nanocomposites [16–19].

However, track membranes have limited applicability in optics due to the low light transmittance in the visible region of 400–760 nm, as well as due to high moisture absorption associated with the features of the molecular structure, namely, the presence of hydrophilic imide rings [20, 21]. It determines the necessity of obtaining

© Cherkashina N.I., Pavlenko V.I., Gorodov A.I., Ryzhikh D.A., Forova E.V., 2023

modified polyimide membranes with a reasonable light transmittance, optical homogeneity, and a hydrophobic surface for creating optical systems [22]. Such a relevance is associated with the technological progress. There is a growing demand for advanced materials. If we consider different polymeric materials, their properties are predetermined by their structure but for some areas they are not functional enough or do not fit the requirements, therefore their application may be limited. Thus, a new direction of composite materials creation is being developing with improved electrical, optical, thermal, mechanical and other properties. By integrating the filler into the pores of track membranes, a composite with the unique properties is obtained, which expands the scope of its application. Nanofillers fill the volume of the polymer due to such processes as polymerization, sol-gel method, mixing of solutions [23], electroforming [24], deposition, and ion exchange. Method depends on the desired result.

It is known that the use of nanofillers in almost any composites can improve the functional characteristics of the material. For example, it was shown in [25] that the introduction of carbon nanofibers in an amount of 1 mass % into a polypropylene matrix makes it possible to increase the bending strength by 22%, the tensile strength by 29%, and the impact strength by 23%. In another paper [26], on the example of bismaleimide/carbon nanotube nanocomposites, it was experimentally demonstrated that the deformation of carbon nanotube bundles (stretching) from 0 to 12% has led to increase in the elastic modulus of mentioned above nanocomposites from 118 to 293 GPa.

In China nanocomposite of polyvinyl alcohol and titanium (IV) isopropoxide has been developed [27]. The nanocomposite has a wide reconfigurable refractive index window of 1.65–1.95 at a wavelength of 550 nm. It has been established that the use of the developed antireflection films in perovskite solar cell modules increases the efficiency of energy conversion from 16.57% to 17.25%.

In Indian researchers have found that the nonlinear optical properties of MoS₂/polyvinyl alcohol nanocomposites can be controlled by changing the concentration of MoS₂ nanoparticles in the polymer matrix, as well as by sonicating a certain concentration at different times. It has been established that with an increase in the concentration of MoS₂ nanoparticles in the polymer matrix, self-focusing transforms into self-defocusing. It is shown in [28] that the introduction of silica filler leads to a significant decrease in the degradation of the optical properties of a polymer composite under the action of vacuum ultraviolet radiation. As nanofillers for polymer composites, both inorganic substances can be used: silica, clay, ceramics; and metals and their oxides: gold, silver, aluminum, iron, cobalt, etc., as well as organic materials, such as carbon nanotubes or graphene [29, 30]. Even though there are many studies on the preparation of composite films and nanofilms, including those based on polyimide [31–35],

an effective method that completely avoids the aggregation of nanoparticles when it is introduced into a polymer, has not yet been identified.

In this research, we have obtained a polymer composite film based on a track membrane, which was filled with silica. We have determined also the possibility of increasing the light transmittance and improving the optical characteristics of the composite film by modifying its surface using laser processing. It is known that the modification with the energy impact of both ionizing radiation and laser processing affects the change in the surface of the processed material properties and allows us to create materials with desired (controlled) properties [36–41].

MATERIALS AND RESEARCH METHODS

The composite material was created on the basis of a polyimide track (nuclear) membrane. The pore diameter is 200 nm, the pore density is $5 \cdot 10^8 \text{ cm}^{-2}$, the thickness of the polyimide membrane is 25 μm (producer it4ip, Belgium). Figure 1 shows SEM images of the original polyimide track (nuclear) membrane on which craters are visible - inlets and outlets, with random arrangement, from a single location to layering. The pores were filled with silica; for the hydrolysis reaction, the following reagents were used: tetraethoxysilane (TEOS) analytical grade TU 2637-187-44493179-2014, glacial acetic acid chemically pure GOST 61-75.

For filling the pores of the track membranes with hydrolysis products we used ultrasonic treatment – an ultrasonic bath TECHMANN® LABORANT model L-22 (manufactured by TEKMANN LLC, Russia). The operating parameters of the ultrasonic bath are presented in the Table 1.

To modify the surface of the composite film, Mini-marker 2-20 A4 PA we used ytterbium pulsed fiber laser (manufactured by LLC Laser Center, Russia). The operating parameters are presented in the Table 2.

Based on the calculation of the reaction equation, the optimal ratios for the hydrolysis reaction were selected. The ratios are presented in the Table 3.

Samples were prepared as follows: track membranes 2×2 cm in size were lowered into weighing bottle and filled with tetraethoxysilane (TEOS) (Fig. 2a, Fig. 2b), further they were being exposed to ultrasound for 30 minutes (Fig. 2c). Further on, according to the Table 3, the rest of the components were added to the bottles, the reaction proceeded in an acidic medium (pH \approx 3) in the presence of a catalyst, acetic acid. Then the samples were being kept in ultrasound for another 1.5 hours at a temperature of 60°C (Fig. 2d). After hydrolysis, the films were washed with distilled water, and large hydrolysis products were removed from the surface. The films were then dried at room temperature and subjected to high-energy laser action.

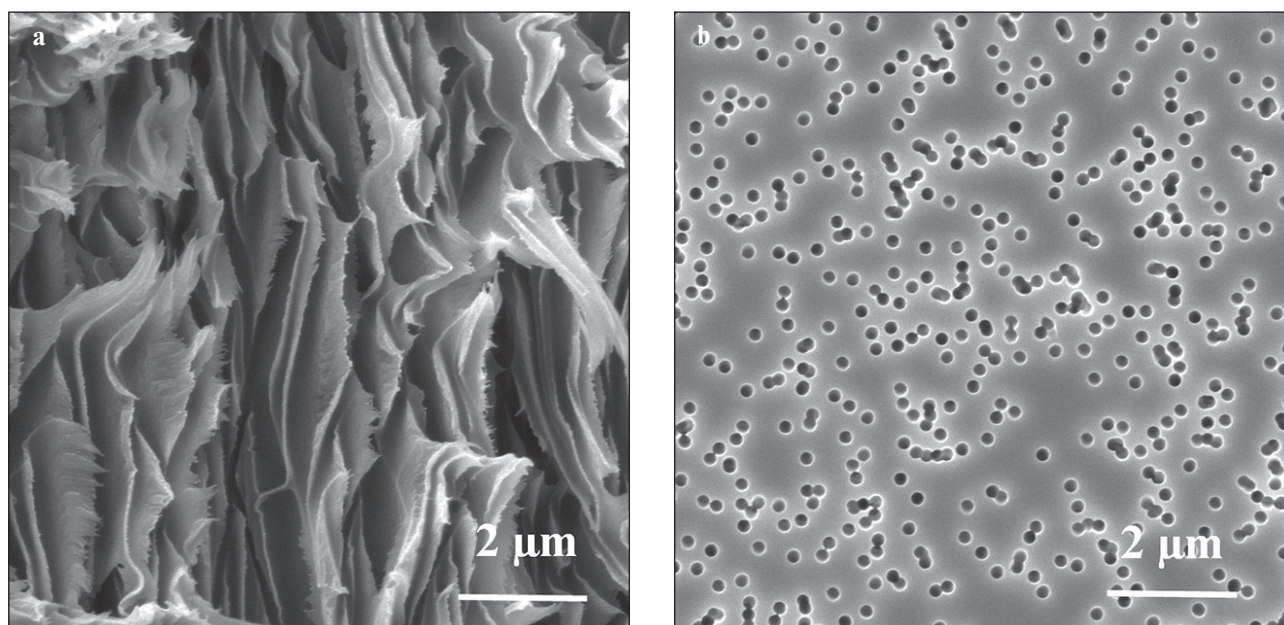


Fig. 1. SEM images of a polyimide track (nuclear) membrane in section (a) and top view (b)

Table 1

Operating parameters of the ultrasonic bath

Parameter	Value
Power, W	90–120
Frequency, kHz	37
Heating, W	120

Table 2

Laser operating parameters

Parameter	Value
Wavelength of the main radiation, nm	1064
Maximum output radiation power, W	20
Maximum energy in a radiation pulse, mJ	1.0

Table 3

Ratio of the components for the hydrolysis reaction

Nature of the catalyst	Ratio of the components with the sequence to their introduction into the solution (water and catalyst are added simultaneously)	
	(C ₂ H ₅ O) ₄ Si, мл	H ₂ O, мл
CH ₃ COOH	35	7

To study the effect of laser processing on composite film samples, 3 processing modes with different power parameters were selected. Modes are presented in the Table 4.

The first sample is unmodified composite film.

To measure the particle size in solution over time, a Zetatrac particle size analyzer (Microtrac Inc, USA) was used. To study the surface morphology of the films, a MIRA3 TESCAN scanning electron microscope (Tescan, Czech Republic) was used. The contact angle of wetting was determined by the sitting drop method using a Krüss DSA30 instrument (Krüss GmbH, Germany). To study changes in the light transmittance and optical density, a LEKI SS1207 spectrophotometer (MEDIORA, Finland) was used. A VERTEX 70 IR-Fourier spectrometer (Bruker Optik GmbH, Germany) was used to measure the optical transmission spectra and intra- and intermolecular interactions of silica and polymers.

RESULTS AND DISCUSSION

As the hydrolysis have been progressing, silica particles have been forming in the solution. At the start of the experiment, the particle size, on average, was 0.00283 μm (Fig. 3), which was 71 times smaller than the pore size. On the above mentioned we suggest that the hydrolysis products have entered the pores and particles continued to grow inside the tracks. This assumption was confirmed by the results of microscopy described below.

Over time, the growth of particles was continuing. The Fig. 4 shows the time point in which the particles have reached an average size of 0.1520 μm. Further, the



Fig. 2. The process of hydrolysis. Sample preparation (a, b), hydrolysis process (c), hydrolysis result (d)

Table 4

Laser sample processing modes

Sample	Number of passes	Power, %	Beam travel speed, mm/s	Modulation frequency, kHz	Pulse duration, ns
1	—	—	—	—	—
2	1	100	85	40	4
3	1	80	85	40	4
4	1	60	85	40	4

growth of the particles continued to an average size of 0.340 μm and 0.480 μm . Further on measurements were not carried out, since the particle size exceeded the pore size track membranes.

As mentioned above, hydrolysis was carried out at a temperature of 60°C due to the proven phenomena that with increasing temperature, the number of forming particles increases, and the reaction proceeds faster. This is explained by the fact that the process of particle formation consists of two stages: the period of induction formation of nuclei and their subsequent growth. During the induction period, there is an increase in concentration

and polymerization into microparticles of molecular SiO_2 , which directly depends on the reaction temperature. Since the hydrolysis reaction rate increases with temperature, the number of microparticles formed during this period also increases, therefore, the number of active collisions during their aggregation increases, which resulting in more formed nuclei. At the second stage, the size of the particles formed during the induction period increases, and there no new formed nuclei.

To study the surface morphology of composite films and their filling with nanosilica, we obtained the results of microscopy and analyzed them (Fig. 5).

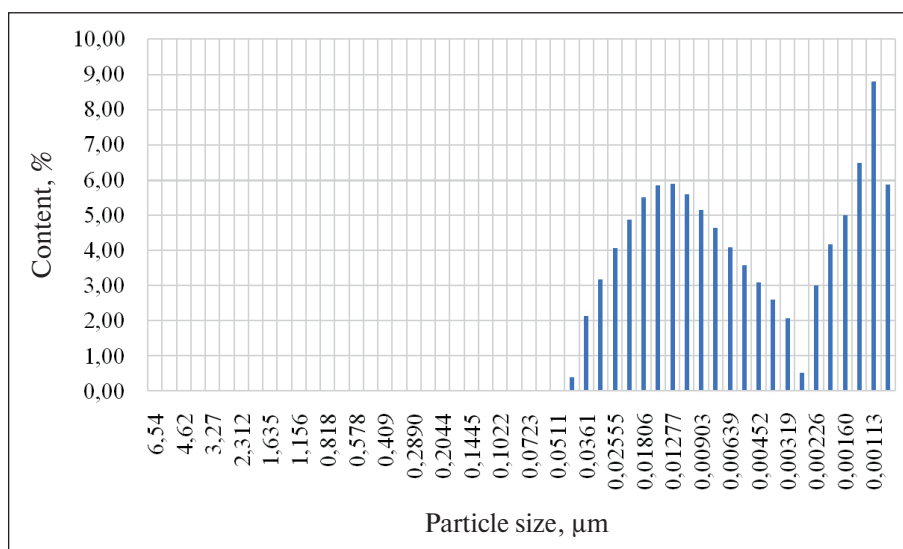


Fig. 3. Forming particles size distribution at the beginning of the experiment

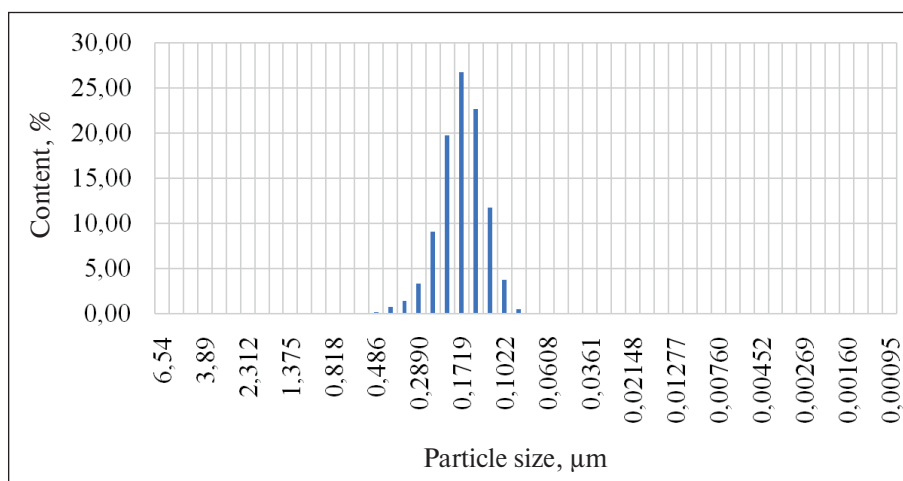


Fig. 4. Forming particles size distribution in the middle of the experiment

According to the SEM images in Figure 1, it can be seen that initially the film has clearly defined holes; the film tracks are hollow in the section. After hydrolysis in the presence of the film, one can observe the filling of tracks with silica (Fig. 5a). The film surface no longer has clearly defined holes, which indicates their filling (Fig. 5a–c). Figures 5 d–f show micrographs of composite membranes irradiated with laser in the second, third and fourth modes from Table 4. The pores of the membranes remain filled, they are not collapsed, silica fills the entire free volume of the tracks. As the laser is passing on, swelling can be observed on the membrane irradiated in the second mode along the beam path (Fig. 5d). A similar effect can also be observed for a film sample irradiated in regime 3 from Table 4 (Fig. 5e). However, as can be seen, the swelling of the membrane is less intense, this is due to the reduced power of impact on the composite film by

20%. Figure 5f shows a composite membrane modified with a laser in the 4th mode from the Table 4. The volume of the membrane is still filled, there are no visible changes, however, no swelling can be seen on the surface of the film, since the laser exposure power is reduced by 40%, in comparison with mode 2 (Fig. 5d).

Similarly, the confirmation that silicon oxide has filled the pore volume is the energy-dispersive analysis data presented in Figure 6. Figure 6 shows the cleavage of a composite track membrane and material's chemical composition, with the filling of the volume with silica.

Figures 7 and 8 show the light absorption spectra of the composite film. The spectra were taken for 4 samples: unmodified composite film and modified composite film laser-irradiated in the modes from the Table 4.

As can be seen from the graphs, the light transmittance of the modified samples has increased. The greatest

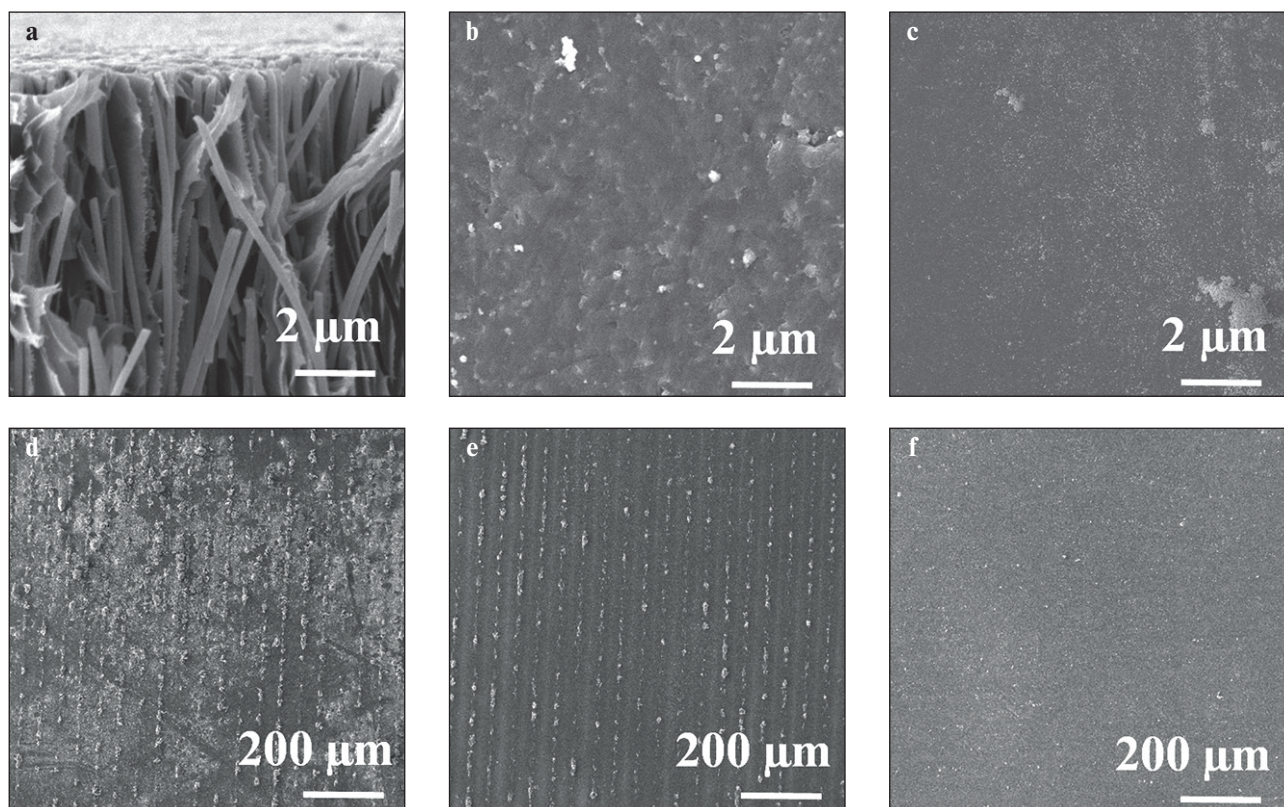


Fig. 5. SEM images of unmodified (a-c) and laser-modified films (d) in mode 2, (e) in mode 3, (f) in mode 4

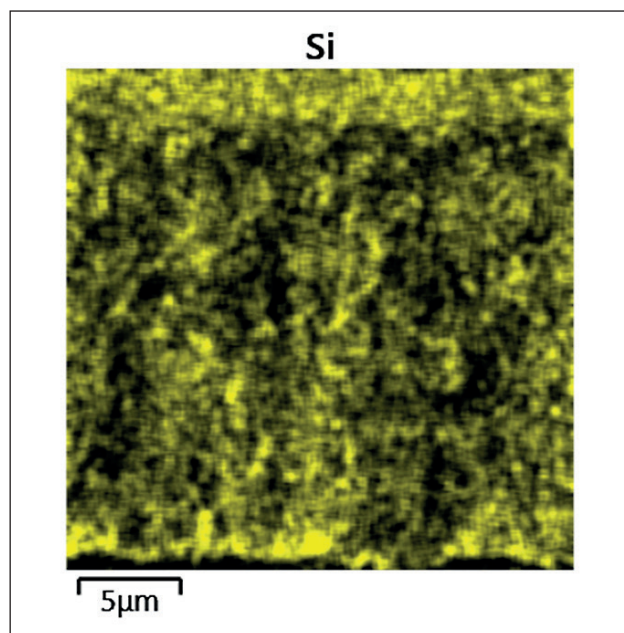


Fig. 6. Energy-dispersive analysis data of composite film cleavage

changes are observed in the visible and infrared spectrum from 500–1000 nm, and in the region of 330–500 nm there are almost no changes between the images – the

light transmittance and optical density of the composite laser-exposed films are closer to the average values of the unmodified membrane.

The greatest changes between unmodified (sample 1) and modified (samples 2–4) composite films are observed at a wavelength of 960 nm, the light transmittance has increased by 92.53%. With decreasing the wavelength, the difference in transmittance is decreasing. The biggest difference at the wavelength of 1000 nm is + 89.97%, at the wavelength of 920 nm is + 82.61%, at 880 nm is + 66.92%, at 840 nm is + 62.82%, at 800 nm is + 57.09%, at 760 nm is + 41.44%.

The optical density of the modified composite films has decreased in comparison with the unmodified ones. The greatest decrease is observed at a wavelength of 960 nm, the optical density has decreased by 20.42%. At the wavelength of 1000 nm it has decreased by 20.39%, at 920 nm it has decreased by 18.60%, at 880 nm it has decreased by 15.86%, at 840 nm it has decreased by 14.62%, at 800 nm it has decreased by 13.08 %, at 760 nm it has decreased by 9.78%.

Figure 9 shows data of IR-spectra for unmodified by laser composite film and high-energy laser-modified film by exposure in the modes from the Table 4. Based on the data obtained, it can be seen that these images have a typical structure for polyimide. The diagram shows absorption bands at 1380–1780 cm^{-1} , which is characteristic of the

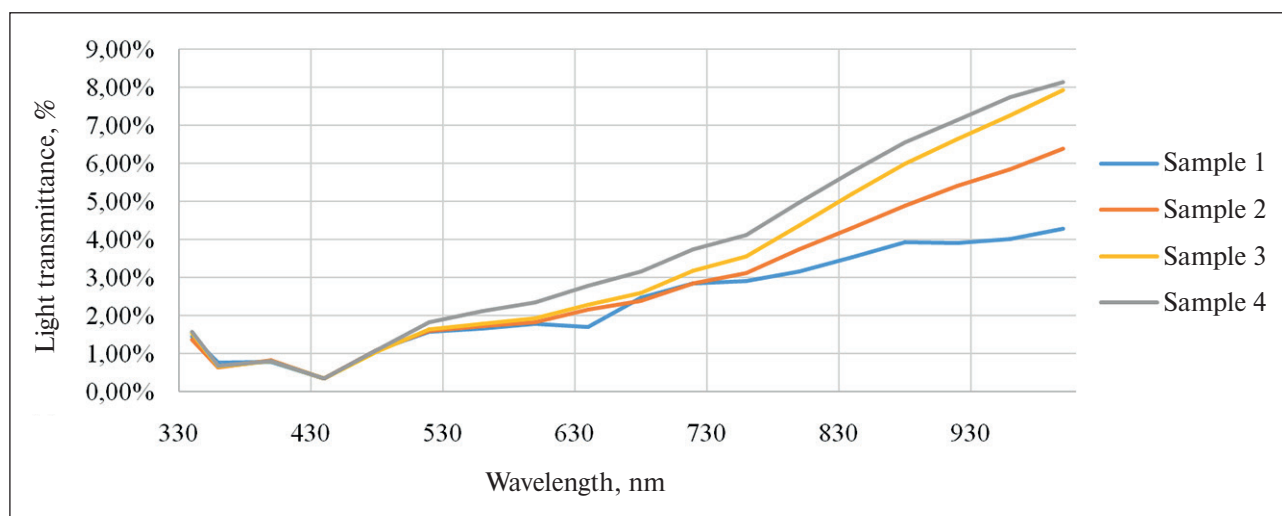


Fig. 7. Light absorption spectra of composite films

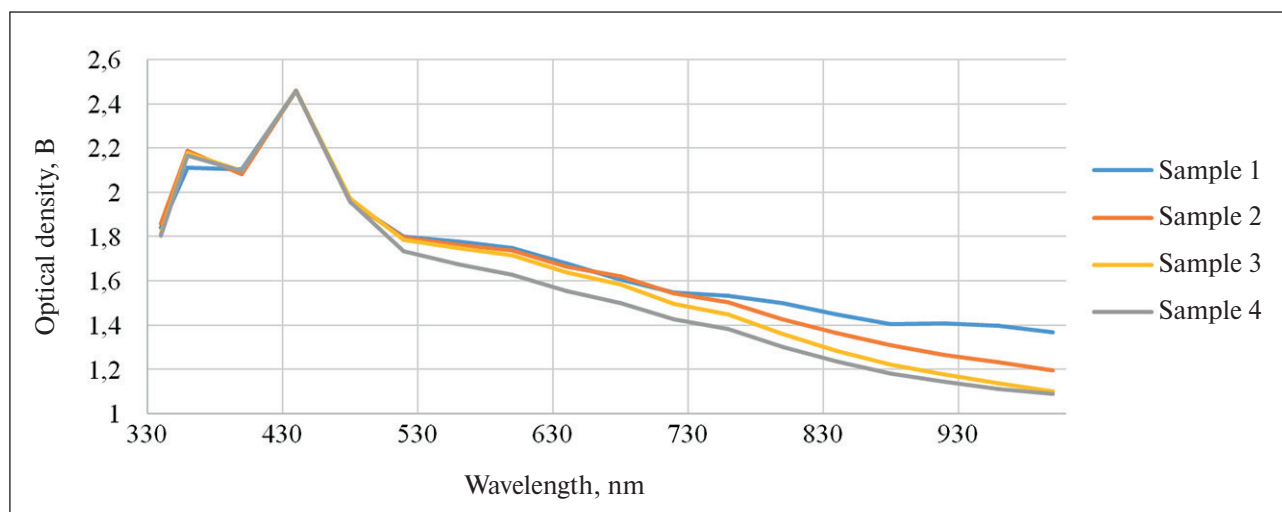


Fig. 8. Light absorption spectra of composite films

imide cycle and oscillation in chemical bonds of the C–N and C=O. A pronounced peak at 1728 cm^{-1} indicates the carbonyl group C=O. The peak at 876 cm^{-1} indicates C–H valence oscillation, and the peak at 1505 cm^{-1} is inherent in C=C valence oscillation.

The ester group is displayed on the Fourier-transform IR spectra as high-intensity bands: in the absorption interval of $1249\text{--}1276\text{ cm}^{-1}$ C–O; the peak at 1126 cm^{-1} indicates valence oscillation C–C(O)–O, this peak is also characteristic of organosilicon compounds and manifests itself when binding ethoxy functional group Si–O–C.

The region $3400\text{--}3500\text{ cm}^{-1}$ indicates the presence of bound hydroxyl groups (water).

Comparative analysis of spectra for laser-modified and laser-unmodified composite films has revealed that no new peaks were formed, and the intensity of the existing peaks has changed after composite films modifica-

tion. There is a decrease in the intensity of the peak at 1728 cm^{-1} and an increase in the intensity of the peaks at 1388 cm^{-1} , 1247 cm^{-1} , 1170 cm^{-1} .

The wettability of the composite films was evaluated by a sitting drop method; wetting was carried out with distilled water and diiodomethane. As is known, polyimides are more hydrophilic than polymers, which is explained by the hydrophilic nature of the imide rings. The need to obtain polyimide membranes with reduced water absorption has been described above. The measuring results for the contact angle of wetting are presented in the Table 5. Figure 10 shows photographs of a water drop on composite films treated with high-energy laser radiation, according to the Table 4. The initial values are extrapolated to zero time.

An analysis of the data obtained shows a trend towards a decrease in the hydrophilicity of the composite film with

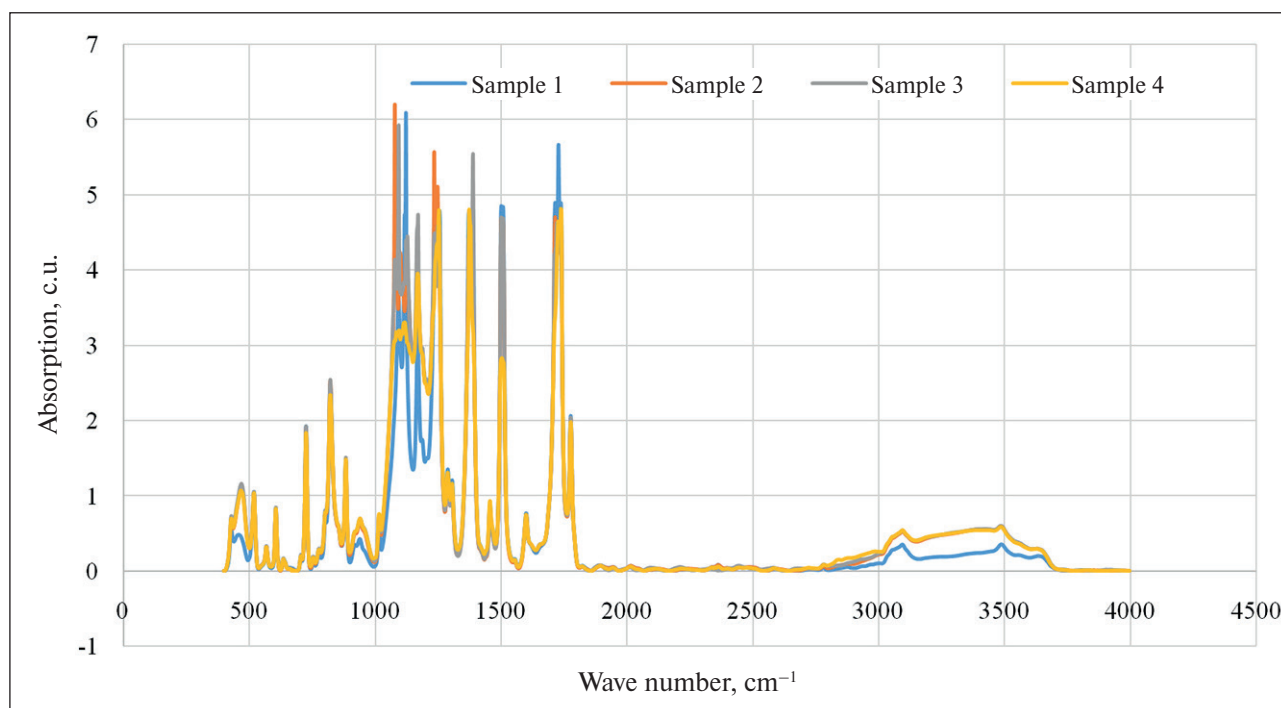


Fig. 9. The Fourier-transform IR spectra of unmodified and laser-modified composite film

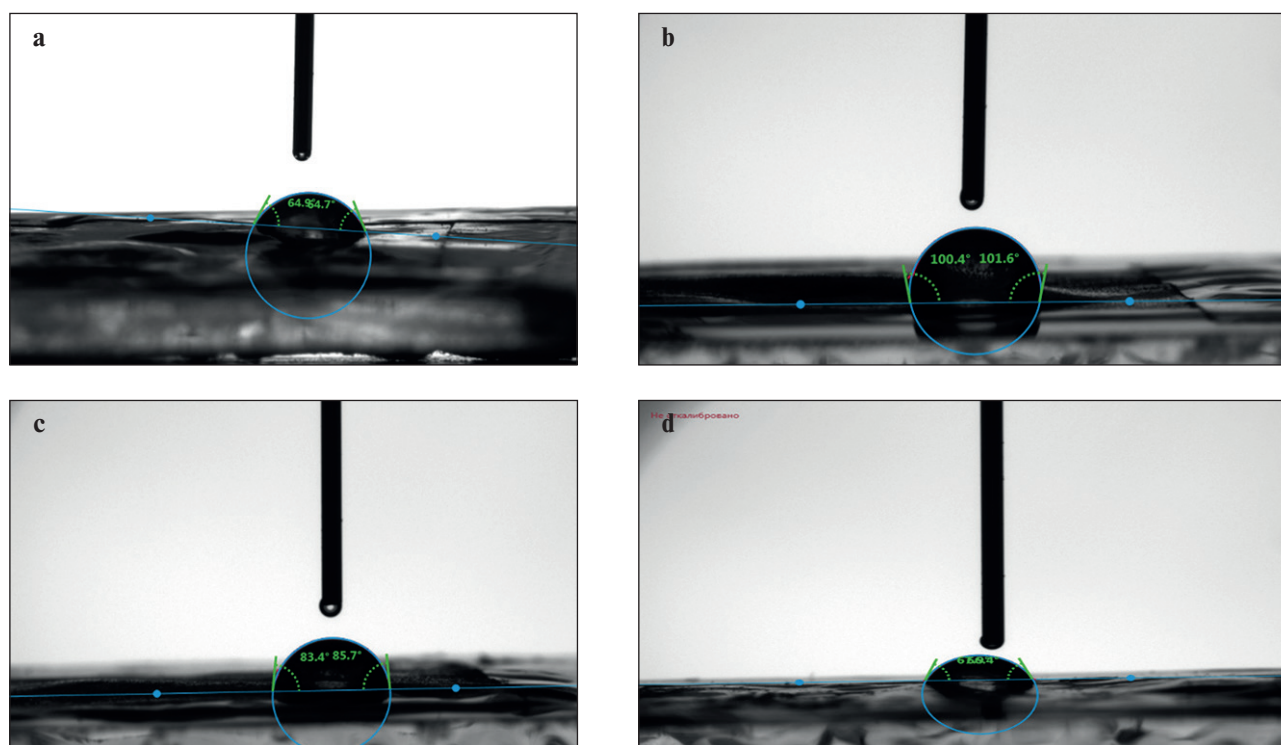


Fig. 10. Photographs of a water drop on unmodified (a) and laser-modified composite film in mode 2 (b), in mode 3 (c), in mode 4 (d)

an increase in the power of impact from 60% to 100%, with other characteristics being equal. The greatest difference in wettability was observed between an unmodified

composite film ($\theta = 66.75 \pm 1.55^\circ$) and membrane irradiated at 100% power ($\theta = 101.52 \pm 3.03^\circ$). The hydrophilic properties of the sample were changed to hydrophobic.

Table 5
Data for contact angle of wetting with water and diiodomethane

Sample	Contact angle of wetting with water. ° (deg.)	Contact angle of wetting with diiodomethane. ° (deg.)
1	66.75 + 1.55	48.51 + 1.05
2	101.52 + 3.03	52.52 + 1.34
3	82.41 + 2.03	52.56 + 1.34
4	70.59 + 1.13	50.57 + 1.85

Thus, the sample irradiated in the second mode from the Table 4 showed an increase in hydrophobicity by 52.01% compared to the unmodified sample; the hydrophilicity of the sample 3 decreased by 23.46% compared to the initial one, and the hydrophilicity of the sample 4 decreased by 5.75%. Data on the free surface energy, dispersed and polar phases are presented in the Table 6.

Surface energy is characterized as the energy of intermolecular interaction of particles at the phase separation boundary with particles of each contacting phase. As can

Table 6
Data on the free surface energy, dispersed and polar phases

Sample	Dispersed phase [mN/m]	Polar phase [mN/m]	Free surface energy [mN/m]
1	35.10 + 2.06	10.47 + 1.27	45.57 + 2.34
2	32.86 + 4.53	2.77 + 1.21	35.63 + 1.51
3	32.83 + 4.50	4.09 + 1.21	36.96 + 1.52
4	33.96 + 1.64	8.89 + 2.01	42.84 + 1.67

REFERENCES

1. Cherkashina N.I., Pavlenko V.I., Noskov A.V. Synthesis and property evaluations of highly filled polyimide composites under thermal cycling conditions from -190°C to $+200^{\circ}\text{C}$. *Cryogenics*. 2019; 104: 102995. <https://doi.org/10.1016/j.cryogenics.2019.102995>
2. Zabegaeva O., Sapozhnikov D., Vygodsky Ya. Molecular composites based on polyimides. *High-molecular compounds*. 2020; 2: 186–199. <https://doi.org/10.31857/S230811472002017X>
3. Ma J., Liu X., Wang R., Lu C., Wen X., Tu G. Research Progress and Application of Polyimide-Based Nanocomposites. *Nanomaterials*. 2023; 13(4): 656. <https://doi.org/10.3390/nano13040656>
4. Malinský P, Romanenko O, Havránek V, Cutroneo M, Novák J, Štěpanovská E, Mikšová R, Marvan P, Mazánek V, Sofer Z, Macková A. Graphene Oxide and Polymer Humidity Micro-Sensors Prepared by Carbon Beam Writing. *Polymers*. 2023; 15(5): 1066. <https://doi.org/10.3390/polym15051066>
5. Yang S.-Y. (Ed.) *Advanced Polyimide Materials: Synthesis, Characterization, and Applications*; Elsevier: Saint Louis, MI, USA; 2018.

be seen from the Table 6, the lower the free energy, the higher the value of the contact angle of wetting.

CONCLUSION

A composite polyimide film based on a polyimide track membrane filled with nanodispersed silicon oxide with improved optical characteristics and water absorption has been created. We have selected optimum modes of exposure to an ytterbium pulsed fiber laser, and have shown the dependence of the exposure power parameter on the properties of a composite film.

The surface modification of the composite material leads to an increase in the contact angle of wetting from $\theta = 66.75 \pm 1.55^{\circ}$ to $\theta = 101.52 \pm 3.03^{\circ}$. Thus, the material acquires hydrophobic properties.

In addition, the modification of films with a laser has a positive effect on the light transmittance of the films, which is increased. The greatest change is observed in the infrared region of emitted spectrum, the average increase in transmission is + 70.48%.

It is necessary to continue research to develop other modes of laser exposure in order to change the characteristics of the filled membrane, which will expand the scope of its application.

6. Gouzman I., Grossman E., Verker R., Atar N., Bolker A., Eliaz N. Advances in Polyimide-Based Materials for Space Applications. *Adv Mater.* 2019; 31(18): 1807738. <https://doi.org/10.1002/adma.201807738>
7. Iwasa R., Suizu T., Yamaji H., Yoshioka T., Nagai K. Gas separation in polyimide membranes with molecular sieve-like chemical/physical dual crosslink elements onto the top of surface. *Journal of Membrane Science.* 2018; 550: 80-90. <https://doi.org/10.1016/j.memsci.2017.12.064>
8. Radzyńska-Lenarcik E, Pyszka I, Urbaniak W. The Use of Polymer Membranes for the Recovery of Copper, Zinc and Nickel from Model Solutions and Jewellery Waste. *Polymers.* 2023; 15(5): 1149. <https://doi.org/10.3390/polym15051149>
9. Kozlovskiy A., Borgekov D., Kenzhina I. et al. PET Ion-Track Membranes: Formation Features and Basic Applications. Nanocomposites, Nanostructures, and Their Applications. NANO 2018. Springer Proceedings in Physics. 2019; 221: 461-479. https://doi.org/10.1007/978-3-030-17759-1_31
10. Pe'py G., Boesecke P., Kuklin A., et al. Cylindrical nanochannels in ion-track polycarbonate membranes studied by small-angle X-ray scattering. *Applied Crystallography.* 2007; 40: 388-392. <https://doi.org/10.1107/S0021889807000088>
11. Tianji Ma, Jean-Marc Janot, Sebastien Balme Track-Etched Nanopore/Membrane: From Fundamental to Applications. *Small Methods.* 2020; 4 (9): 2000366. <https://doi.org/10.1002/smt.202000366>
12. Jian-Xin Yang, Zhi-Bo He, Shi-Lun Guo Identification and harmfulness analysis of solid particles contained in medical injections and their removal by nuclear track membranes. *Perspectives in Science.* 2019; 12: 100399. <https://doi.org/10.1016/j.pisc.2019.100399>
13. Nana Jin, Li Xue, Ying Ding, Yingjia Liu, Fan Jiang, Ming Liao, Yanbin Li, Jianhan Lin A microfluidic biosensor based on finger-driven mixing and nuclear track membrane filtration for fast and sensitive detection of Salmonella. *Biosensors and Bioelectronics.* 2023; 220: 114844. <https://doi.org/10.1016/j.bios.2022.114844>
14. Zhi-Bo He, S.-L. Guo, Applications of Nuclear Track Membranes to Filtration of Medical Injections and Various Transfusions to Remove Solid Particles. *Physics Procedia.* 2015; 80: 131-134. <https://doi.org/10.1016/j.phpro.2015.11.081>
15. Bositykh E., Sokhoreva V., Pichugin V. Investigation of the possibility of using nuclear track membranes for ophthalmology. *Membranes and membrane technologies.* 2014; 4 (4): 267.
16. Calvo J.I., Bottino A., Capannelli G., Hernández A. Comparison of liquid–liquid displacement porosimetry and scanning electron microscopy image analysis to characterise ultrafiltration track-etched membranes. *Journal of Membrane Science.* 2004; 239 (2): 189-197. <https://doi.org/10.1016/j.memsci.2004.02.038>
17. Vinogradov I., Nechaev A., Rossow A. Composite membranes based on a track membrane and chitosan nanoframeworks. Science of Russia: Goals and objectives. *Collection of scientific papers based on the materials of the XXVII International Scientific and Practical Conference.* June 10, 2021. 2021; 152. <https://doi.org/10.18411/sr-10-06-2021-26>
18. Khlebnikov N.A., Polyakov E.V., Borisov S.V., Shepatkovskii O.P., Krasil'nikov V.N. Application of Nanocomposite Track Membranes for Electron Microscopy Samples Preparation. *Advanced Materials Research.* 2014; 1082: 51–56. <https://doi.org/10.4028/www.scientific.net/amr.1082.51>
19. Al Harby NF, El-Batouti M, Elewa MM. Prospects of Polymeric Nanocomposite Membranes for Water Purification and Scalability and their Health and Environmental Impacts: A Review. *Nanomaterials.* 2022; 12(20): 3637. <https://doi.org/10.3390/nano12203637>
20. Wu T., Dong J., Gan F., Fang Y., Zhao X., Zhang Q. Low dielectric constant and moisture-resistant polyimide aerogels containing trifluoromethyl pendent groups. *Applied Surface Science.* 2018; 440: 595–605. <https://doi.org/10.1016/j.apsusc.2018.01.132>
21. Yin J, Mao D, Fan B. Copolyamide-Imide Membrane with Low CTE and CME for Potential Space Optical Applications. *Polymers.* 2021; 13(7): 1001. <https://doi.org/10.3390/polym13071001>
22. Mao D., Lv G., Gao G., Fan B. Fabrication of polyimide films with imaging quality using a spin-coating method for potential optical applications. *Journal of Polymer Engineering.* 2019; 39(10): 917–925. <https://doi.org/10.1515/polyeng-2019-0177>
23. Jiang H., Xu L., Chen G., Fang X. Aqueous Solution Blending Route for Preparing Flexible and Antistatic Polyimide/Carbon Nanotube Composite Films with Core-Shell Structured Polyimide/Graphene Microspheres. *Polym. Compos.* 2022; 43: 6062–6073.
24. Zhou X., Ding C., Cheng C., Liu S., Duan G., Xu W., Liu K., Hou H. Mechanical and Thermal Properties of Electrospun Polyimide/Rgo Composite Nanofibers Via in-Situ Polymerization and in-Situ Thermal Conversion. *European Polymer Journal.* 2020; 141: 110083. <https://doi.org/10.1016/j.eurpolymj.2020.110083>

25. Mainnikova N., Yarmizina A., Trofimov D., Kostromina N., Kravchenko T., Yakovleva K. Investigation of the effect of carbon nanofillers on the properties of composites based on polypropylene. *Plastic masses*. 2020; 3-4: 23–25. <https://doi.org/10.35164/0554-2901-2020-3-4-23-25>
26. Kozlov G., Dolbin I. Comparative analysis of the effectiveness of carbon nanotubes and graphene in the reinforcement of polymer nanocomposites. *Journal of technical physics*. 2020; 62(8): 1240–1243. <https://doi.org/10.21883/FTT.2020.08.49608.078>
27. Huo M., Hu Y., Xue Q., Huang J, Xie G. Solution-Processed Large-Area Organic/Inorganic Hybrid Antireflective Films for Perovskite Solar Cell. *Molecules*. 2023; 28(5): 2145. <https://doi.org/10.3390/molecules28052145>
28. Pavlenko V.I., Zabolotny V.T., Cherkashina N.I., Edamenko O.D. Effect of vacuum ultraviolet on the surface properties of high-filled polymer composites. *Inorganic Materials: Applied Research*. 2014; 5(3): 219–223. <https://doi.org/10.1134/S2075113314030137>
29. Hsiao Y.-S., Chang-Jian C.-W., Uang T.-Y., Chen Y.-L., Huang C.-W., Huang J.-H., Wu N.-J., Hsu S.-C., Chen C.-P. Lightweight Flexible Polyimide-Derived Laser-Induced Graphenes for High-Performance Thermal Management Applications. *Chemical Engineering Journal*. 2023; 451(3): 138656. <https://doi.org/10.1016/j.cej.2022.138656>
30. Pavlenko V.I., Cherkashina N.I. Synthesis of hydrophobic filler for polymer composites. *International Journal of Engineering and Technology*. 2018; 7(2): 493–495. <https://doi.org/10.14419/ijet.v7i2.23.15341>
31. Xing S., Pan Z. Wu X., Chen H., Lv X., Li P., Liu J., Zhai J. Enhancement of Thermal Stability and Energy Storage Capability of Flexible Ag Nanodot/Polyimide Nanocomposite Films Via in Situ Synthesis. *Journal of Materials Chemistry*. 2020; 8(36): 12607–12614. <https://doi.org/10.1039/D0TC02516J>
32. Yadav D., Borpatra G. M., Karki S., Ingole P.G. A Novel Approach for the Development of Low-Cost Polymeric Thin-Film Nanocomposite Membranes for the Biomacromolecule Separation. *ACS Omega*. 2022; 7(51): 47967–47985. <https://doi.org/10.1021/acsomega.2c05861>
33. Borpatra Gohain M., Karki S., Yadav D., Yadav A., Thakare N.R., Hazarika S., Lee H.K., Ingole P.G. Development of Antifouling Thin-Film Composite/Nanocomposite Membranes for Removal of Phosphate and Malachite Green Dye. *Membranes*. 2022; 12(8): 768. <https://doi.org/10.3390/membranes12080768>
34. Nam V.B., Shin J., Choi A., Choi H., Ko S.H., Lee D. High-Temperature, Thin, Flexible and Transparent Ni-Based Heaters Patterned by Laser-Induced Reductive Sintering on Colorless Polyimide. *Journal of Materials Chemistry*. 2021; 9(17): 5652–5661. <https://doi.org/10.1039/D1TC00435B>
35. Zhang Y., Ma Z., Ruan K., Gu J. Multifunctional $Ti_3C_2Tx-(Fe_3O_4/Polyimide)$ Composite Films with Janus Structure for Outstanding Electromagnetic Interference Shielding and Superior Visual Thermal Management. *Nano Research*. 2022; 15(6): 5601–5609. <https://doi.org/10.1007/s12274-022-4358-7>
36. Jun Xu, Guojun Zhang, Congyi Wu, Weinan Liu, Tian Zhang, Yu Huang, Youmin Rong Organic solvent assisted laser processing of transparent polymer films based on the swelling and penetration behavior. *Optics & Laser Technology*. 2022; 150: 107937. <https://doi.org/10.1016/j.optlastec.2022.107937>
37. Yastrebinsky R.N., Pavlenko V.I., Matukhin P.V., Cherkashina N.I., Kuprieva O.V. Modifying the surface of iron-oxide minerals with organic and inorganic modifiers. *Middle East Journal of Scientific Research*. 2013; 18(10): 1455–1462. <https://doi.org/10.5829/idosi.mejsr.2013.18.10.7098>
38. Anwer G., Acherjee B. Laser polymer welding process: Fundamentals and advancements. *Materials Today: Proceedings*. 2022; 61(1): 34–42. <https://doi.org/10.1016/j.matpr.2022.03.307>
39. Matyukhin P.V., Pavlenko V.I., Yastrebinsky R.N., Cherkashina N.I. The high-energy radiation effect on the modified iron-containing composite material. *Middle East Journal of Scientific Research*. 2013; 17 (9): 1343–1349. <https://doi.org/10.5829/idosi.mejsr.2013.17.09.70100>
40. Mishra L., Mishra D., Mahapatra T.R. Optimization of process parameters in Nd:YAG laser micro-drilling of graphite/epoxy based polymer matrix composite using Taguchi based Grey relational analysis. *Materials Today: Proceedings*. 2022; 62(14): 7467–7472. <https://doi.org/10.1016/j.matpr.2022.03.501>
41. Dahmen M., Vedder C., Baek S., Stollenwerk J. Dual-beam laser-based processing of tribological polymer coatings. *Procedia CIRP*. 2022; 11: 257–260. <https://doi.org/10.1016/j.procir.2022.08.061>

INFORMATION ABOUT THE AUTHORS

Natalia I. Cherkashina – Dr. Sci. (Eng.), Associate Professor, Leading Researcher, Head of the Research Laboratory «Development of scientific and technical foundations for the creation of polymer systems from renewable plant materials», Belgorod State Technological University named after V.G. Shukhov, Belgorod, Russia, natalipv13@mail.ru, <https://orcid.org/0000-0003-0161-3266>

Vyacheslav I. Pavlenko – Dr. Sci. (Eng.), Professor, Head of the Department «Theoretical and Applied Chemistry», Belgorod State Technological University named after V.G. Shukhov, Belgorod, Russia, belpavlenko@mail.ru, <https://orcid.org/0000-0002-3464-1880>

Andrey I. Gorodov – Cand. Sci. (Eng.), Associate Professor, Department of «Theoretical and Applied Chemistry», Belgorod State Technological University named after V.G. Shukhov, Belgorod, Russia, gorodov-andrey@mail.ru, <https://orcid.org/0000-0002-5530-3282>

Daria A. Ryzhikh – Jun. Res. Postgraduate student of the Department of «Theoretical and Applied Chemistry», Belgorod State Technological University named after V.G. Shukhov, Belgorod, Russia, sinebokd@mail.ru, <https://orcid.org/0000-0002-8886-6022>

Elena V. Forova – Research Engineer at the Research Laboratory «Development of scientific and technical foundations for the creation of polymer systems from renewable plant materials», Belgorod State Technological University named after V.G. Shukhov, Belgorod, Russia, unir.bstu@gmail.com <https://orcid.org/0000-0001-7510-3547>

CONTRIBUTION OF THE AUTHORS

Natalia I. Cherkashina – scientific guidance; setting up goals and objectives of the research; research results analysis; revision of the text.

Vyacheslav I. Pavlenko – experimental work planning; research results analysis; conclusions of the article.

Andrey I. Gorodov – development of the research methodology; research results analysis; graphical and tabular presentation of results.

Daria A. Ryzhikh – conducting the experimental part of the study; research results analysis; graphical and tabular presentation of the results; writing the original text of the article.

Elena V. Forova – literature review; conducting the experimental part of the study

The authors declare no conflicts of interests.

The article was submitted 28.02.2023; approved after reviewing 27.03.2023; accepted for publication 31.03.2023.